Archiv der Pharmazie

DPhG

FULL PAPER OPEN ACCESS

Structure Characterization and Antibacterial, Antifungal, and Antiquorum-Sensing Activity of New Metabolites From the Lipophilic Fractions of *Platycodon grandiflorum* Root

Hyukbean Kwon[1] | Jimin Moon[1] | Jeong-Hyeon Kim[2] | Prima F. Hillman[3] | Silviani Velina[1,4] | Joo-Won Nam[1] | Sang-Jip Nam[2] | Inho Choi[4,5] | Kyung Sik Song[6] | Geum Jin Kim[7] | Hyukjae Choi[1,4]

[1]College of Pharmacy, Yeungnam University, Gyeongsan, Gyeong-buk, Republic of Korea | [2]Department of Chemistry and Nanoscience, Ewha Womans University, Seoul, Republic of Korea | [3]Department of Chemistry, Faculty of Mathematics and Natural Sciences, Universitas Andalas, Kampus Limau Manis, Padang, Indonesia | [4]Research, Institute of Cell Culture, Yeungnam University, Gyeongsan, Gyeong-buk, Republic of Korea | [5]Department of Medical Biotechnology, Yeungnam University, Gyeongsan, Gyeong-buk, Republic of Korea | [6]Research, Institute of Pharmaceutical Sciences, College of Pharmacy, Kyungpook National University, Daegu, Republic of Korea | [7]Department of Pharmacology, School of Medicine, Dongguk University, Gyeongju, Gyeong-buk, Republic of Korea

Correspondence: Geum Jin Kim (geumjinkim@dongguk.ac.kr) | Hyukjae Choi (h5choi@yu.ac.kr)

Received: 22 February 2025 | **Revised:** 6 June 2025 | **Accepted:** 14 June 2025

Funding: This study was supported by the Basic Science Research Program of the National Research Foundation of Korea (NRF) grants funded by the Korean government (MSIT) (Grant No. NRF-2020R1A6A1A03044512, and NRF-2021R1A2C1010727), [Cooperative Research Program for Agriculture Science & Technology Development (PJ014208032023) funded by Rural Development Administration] and Yeungnam University research grant funded by Yeungnam University.

Keywords: antimicrobial | antiquorum-sensing | lipophilic fraction | *Platycodon grandiflorum* | polyacetylene

ABSTRACT

The root of *Platycodon grandiflorum* has long been used as a vegetable and traditional medicine. Although the antibacterial activity of the plant's lipophilic (hexanes and dichloromethane) fractions has been reported, the specific antibacterial compounds have not been identified. In this study, chemical analysis of the lipophilic fractions of *P. grandiflorum* extracts led to the discovery of five new polyacetylenes (**1**–**5**) and nine known compounds (**6**–**14**). Their structures were elucidated and confirmed based on 1D and 2D NMR data together with mass spectra. In particular, the relative and absolute configurations of **1** were elucidated by coupling constants, NOESY and *J*-based configurational analysis in combination with Mosher's method. Compounds **1** and **2** demonstrated strong antifungal activity against *Candida albicans*. Additionally, compound **1** significantly inhibited quorum sensing in *Chromobacterium violaceum*, a commonly used biosensor strain. Compounds **2** and **14** also exhibited mild inhibitory activity. Compounds **8** and **12**–**14** exhibited potent antibacterial activity against *Escherichia coli*, *Kocuria rhizophila*, and *Staphylococcus aureus*, as well as antifungal activity against *Candida albicans*. These compounds may be responsible of the antimicrobial activity of *P. grandiflorum*.

1 | Introduction

Platycodon grandiflorum is an herbaceous perennial plant in the family Campanulaceae, widely distributed in East Asia. The root of *P. grandiflorum* is a common vegetable and traditional medicine in Korea, China, and Japan. As a vegetable in Korean cuisine, it is called Doraji and used as raw material in cooking or for wine and tea preparation, with its characteristic flavor

Hyukbean Kwon and Jimin Moon contributed equally to this study.

and bitter taste. Additionally, it is used in traditional medicine (Platycodonis radix) to treat colds, coughs, sore throats, upper respiratory infections, tonsillitis, and chest congestion in East Asia [1]. To date, many natural products from this plant have been reported, including triterpene saponins, polysaccharides [2], flavonoids [3, 4], phenolic acids [5], polyacetylenes [6–8], and sterols [9]. Triterpenoid saponins, such as platycodin D, are the major bioactive components of Platycodonis radix, with over 60 triterpene saponins reported [10]. Extracts from this plant have shown antitumor [11, 12], antitussive [1], anti-inflammatory [13], antiobesity [14], antifibrosis [15], antioxidant [16], hepatoprotective [17], blood lipid-lowering [18], immune-modulatory [19], and antibacterial [20] activities. Most of these pharmacological activities are attributed to triterpene saponins and polysaccharides [10]. However, the compound responsible for the antibacterial activity of *P. grandiflorum* remains unknown. Previously, lipophilic extracts were reported to have antibacterial and antifungal activities [21].

In our preliminary study, a 70% ethanolic extract of *P. grandiflorum* and its hexanes fraction showed antibacterial activity against *Staphylococcus aureus* KCTC1927 and *Escherichia coli* KCTC2441 (Supporting Information S1: Table S1). Thus, the lipophilic (hexanes and dichloromethane) fractions of *P. grandiflorum* extracts were selected for chemical investigation, leading to the isolation of five novel polyacetylenes (**1**–**5**), along with nine known compounds (**6**–**14**), and the discovery of antimicrobial compounds among the isolates (Figure 1). Extensive inspection of 1D and 2D NMR data, together with *J*-based configuration analysis for **1**, was conducted to elucidate its planar structure with relative configurations. The absolute configurations of **1** were determined using advanced Mosher's analysis. Furthermore, the antibacterial, antifungal, and quorum-sensing inhibitory activities of isolates (**1**–**2**, **5**–**14**) were evaluated to uncover the principles of the antimicrobial activities of *P. grandiflorum*.

2 | Results and Discussion

2.1 | Structural Elucidation

Platypyran A (**1**) was isolated as a brown oil. Its molecular formula, $C_{14}H_{18}O_2$, was determined by a protonated ion peak at

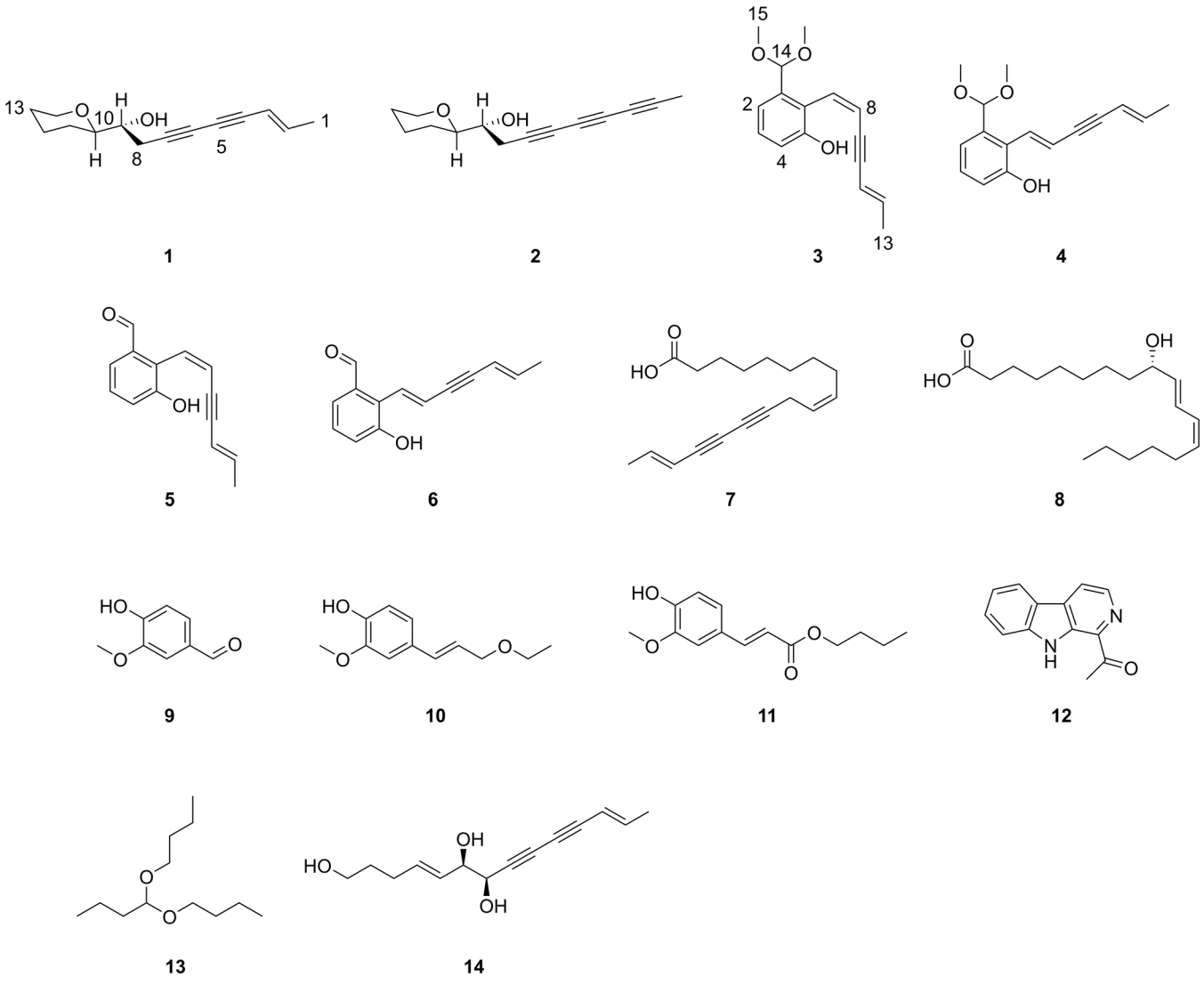

FIGURE 1 | Structures of compounds (**1**–**14**) isolated from the roots of *Platycodon grandiflorum*.

m/z 219.1391 $[M + H]^+$ in the HR–FAB–MS spectrum, indicating six degrees of unsaturation (Supporting Information S1: Figure S1). The analysis of ^1H and ^{13}C NMR, along with phase-edited HSQC spectra, allowed for the assignment of H–C connectivity and the protonation of each carbon. The data revealed two olefinic methines (δ_C 143.5/δ_H 6.29; δ_C 109.9/δ_H 5.50), two oxygenated methanetriyl group (δ_C 78.7/δ_H 3.36; δ_C 72.7/δ_H 3.58), one oxygenated methylene (δ_C 68.7/δ_H 3.46, 4.01), four nonoxygenated methylenes (δ_C 27.8/δ_H 1.44, 1.57; δ_C 26.0/δ_H 1.53; δ_C 24.4/δ_H 2.53, 2.62; δ_C 23.1/δ_H 1.53, 1.87), a methyl group (δ_C 19.0/δ_H 1.80), and four nonprotonated carbons (δ_C 79.6, 76.9, 74.5, and 67.0) (Table 1). Analysis of 1D and 2D NMR (HSQC, COSY and HMBC) data, enabled the construction of partial structures (Supporting Information S1: Figures S2–S6). COSY correlations of H-2 (δ_H 6.29) with H-1 (δ_H 1.80), and H-3 (δ_H 5.50) suggested a propene fragment, supported by HMBC correlations from H-1 to C-2 (δ_C 143.5) and C-3 (δ_C 109.9). A series of COSY correlations from H-8 to H-14 via H-9, H-10, H-11, H-12, and H-13, along with HMBC correlations from H-14 (δ_H 3.46 and 4.01) to C-10 (δ_C 78.7), suggested the presence of a 1-(tetrahydro-2*H*-pyran-2-yl)ethanol spin system. The two partial structures were connected via a diyne linkage based on the long-range HMBC correlations from H-1 to C-4 (δ_C 74.5)/C-6 (δ_C 67.0)/C-7 (δ_C 79.6)/C-9 (δ_C 72.7), from H-2 (δ_H 6.29) to C-4 (δ_C 74.5)/C-6 (δ_C 67.0), from H-3 (δ_H 5.50) to C-4 (δ_C 74.5)/C-6 (δ_C 67.0)/C-7 (δ_C 79.6)/C-9 (δ_C 72.7), from H-8a (δ_H 2.53) to C-2 (δ_C 143.5)/C-3 (δ_C 109.9)/C-4 (δ_C 74.5)/C-6 (δ_C 67.0)/C-7 (δ_C 79.6)/C-9 (δ_C 72.7), and from H-8b (δ_H 2.62) to C-2 (δ_C 143.5)/C-3 (δ_C 109.9)/C-4 (δ_C 74.5)/C-6 (δ_C 67.0)/C-7 (δ_C 79.6)/C-9 (δ_C 72.7). Additionally, the vicinal ^1H–^1H coupling at $^3J_{H\text{-}2,H\text{-}3}$ measured at 15.9 Hz, suggested a *trans* configuration for the olefin. These data resulted in the planar structure of **1** (Figure 2). The relative configuration between C-9 and C-10 was determined through analysis of vicinal ^1H–^1H coupling constants, NOESY spectra, and *J*-based configuration analysis [22]. The two large vicinal ^1H–^1H couplings between H-10 and H-11b (11.1 Hz) and between H-13b and H-14a (11.2 Hz) indicate that these protons are all axially oriented. The relatively small vicinal ^1H–^1H couplings between H-10 an H-11a (2.1 Hz), between H-13a and H-14a (2.8 Hz), between H-13a and H-14b (2.3 Hz), and between H-13b and H-14b (2.3 Hz) indicated that H-11a, H-13a, and H-14b are in equatorial orientations. The NOESY cross-peak between H-11b and H-13b further supported their axial positioning (Figure 2 and Supporting Information S1: Figure S7).

The ^1H-^{13}C heteronuclear coupling constants were measured through HETLOC experiments (Supporting Information S1: Figure S8). The key ^1H–^1H vicinal coupling constant at $^3J_{H\text{-}9,H\text{-}10}$ was evaluated at 5.6 Hz, indicating a medium-range coupling consistent with the equilibrium between *anti*- and *gauche*-rotamers. Additionally, the two relatively small $^3J_{H,C}$ values between H-9 and C-11 (1.2 Hz) as well as between C-8 and H-10 (2.4 Hz), along with the two medium $^2J_{H,C}$ values between H-9 and C-10 (−1.5 Hz) as well as C-9 and H-10 (−2.1 Hz), suggested that C-9/C-10 adopt a *threo* form, with the two major rotamers being A-1 and A-3 (Figure 3). This was further supported by NOESY correlations: from H-10 to

TABLE 1 | ^1H NMR data at 600 MHz and ^{13}C NMR data at 150 MHz of compounds **1** and **2** in $CDCl_3$ (δ in ppm, *J* in Hz).

	Compound 1		Compound 2	
No.	δ_C	δ_H	δ_C	δ_H
1	19.0	1.80 dd (6.9, 1.4)	4.5	1.95 s
2	143.5	6.29 dq (15.9, 6.9)	75.2	
3	109.9	5.50 dq (15.9, 1.4)	64.9	
4	74.5		59.6	
5	76.9[a]		60.9	
6	67.0		67.3	
7	79.6		75.1	
8	24.4	2.53 dd (17.3, 5.6)	24.1	2.50 dd (17.4, 5.6)
		2.62 dd (17.3, 5.6)		2.59 dd (17.4, 5.6)
9	72.7	3.58 q (5.6)	72.4	3.58 p (5.6)
10	78.7	3.36 ddd (11.1, 5.6, 2.1)	78.5	3.34 ddd (11.1, 5.6, 2.1)
11	27.8	1.44 m	27.6	1.45 m
		1.57 m		1.56 m
12	26.0	1.53 m[b]	25.9	1.53 m[b]
13	23.1	1.53 m[b]	22.9	1.53 m[b]
		1.87 m		1.88 m
14	68.7	3.46 td (11.2, 2.8)	68.6	3.46 td (11.1, 2.7)
		4.01 dt (11.2, 2.3)		4.01 dt (11.1, 2.2)
9-OH				2.60 brs[b]

[a]Assigned by HMBC.
[b]Overlapped signals.

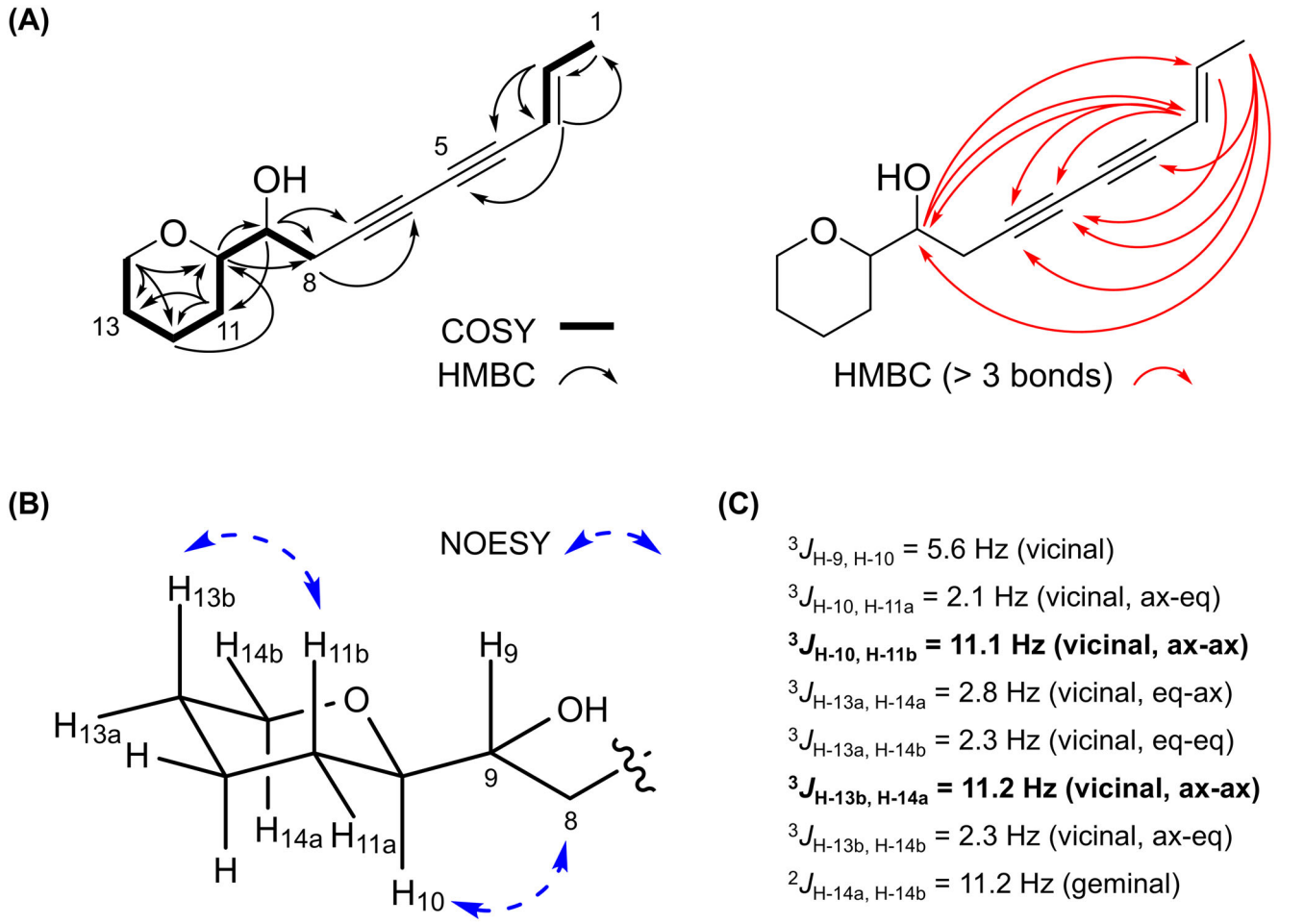

FIGURE 2 | Key 2D NMR correlations of **1**. (A) Planar structure of **1** with key COSY and HMBC correlations. (B) Key NOESY correlations. (C) ^{1}H–^{1}H coupling constants based on proton assignment of axial-equatorial orientation on a pyran ring structure of **1**. (D) Zoomed in ^{1}H NMR spectra of H-9, H-10, H-14a, and H-14b.

H-8a/H-8b/H-9 and from H-9 to H-11a/H-11b for the A-1 rotamer; from H-8 to H-10/H-11b, and from H-9 to H-11a/H-11b for the A-3 rotamer (Figure 3). Comparison of ^{1}H NMR data with previously reported synthetic model compounds showed strong agreement with the *threo* configuration [23]. The absolute configuration of compound **1** was determined using the advanced Mosher's method, and the $\Delta\delta_{S-R}$ values indicated the *R* configurations for both C-9 and C-10 (Figure 4) [24]. Consequently, the absolute configuration of compound **1** was unambiguously established as 2*E*, 9*R*, and 10*R*.

Platypyran B (**2**) was isolated as yellow oil. The molecular formula of **2** was determined as $C_{14}H_{16}O_2$ by an ion peak of protonated molecule at *m/z* 217.1228 $[M+H]^+$ in the HR–FAB–MS spectrum, indicating 7 degrees of unsaturation in **2** (Supporting Information S1: Figure S9). The similarities in the ^{1}H NMR spectrum, along with mass spectrometry data, suggested a structural resemblance between compounds **2** and **1** (Table 1). The distinctive differences in the ^{1}H and ^{13}C NMR spectra of **2** from those of **1** were the absence of signals from a double bond and the presence of two additional unprotonated

Observed ^3J and ^2J in Hz	A-1 /A-2	A-2 /A-3	**A-1 /A-3**	B-1 /B-2	B-2 /B-3	B-1 /B-3
$^3J_{H\text{-}10,\ H\text{-}9}$ = 5.6 (M)	S	M	M	S	M	M
$^3J_{H\text{-}10,\ C\text{-}8}$ = 2.4 (S)	M	M	S	M	S	M
$^3J_{C\text{-}11,\ H\text{-}9}$ = 1.2 (S)	M	M	S	M	M	S
$^2J_{C\text{-}10,\ H\text{-}9}$ = -1.5 (M)	M	L	M	M	L	M
$^2J_{H\text{-}10,\ C\text{-}9}$ = -2.1 (M)	M	L	M	M	M	L

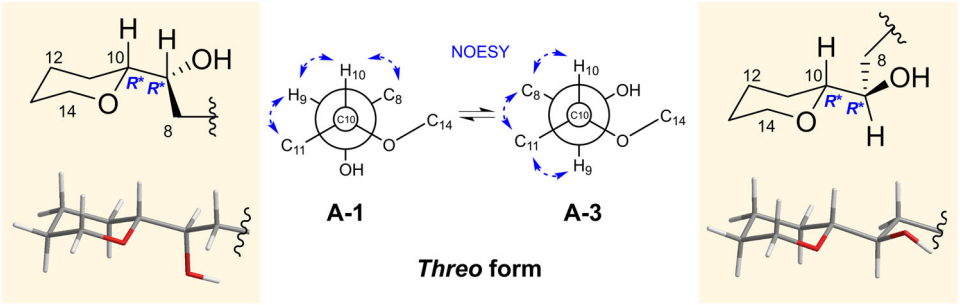

FIGURE 3 | Approaches for determination of relative configurations at C9–C10 of **1**. Comparison data of homo- and hetero-nucleus coupling constants with *J*-based configuration analysis (JBCA) models. Newman projections for C-10/C-9 by analysis result of JBCA.

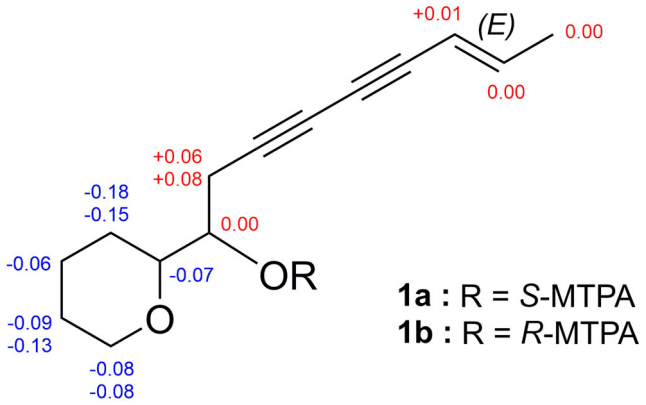

FIGURE 4 | $\Delta\delta_{S-R}$ values of the MTPA esters of **1** in pyridine-d_5.

carbons at δ_C 75.2 and δ_C 64.9. Extensive 1D and 2D NMR data analysis (Supporting Information S1: Figures S10–S14) suggested that compound **2** had a triyne structure, as shown in Figure 1. The key HMBC correlations from H-1 (δ_H 1.95) to C-2 (δ_C 75.2)/C-3 (δ_C 64.9)/C-4 (δ_C 59.6)/C-6 (δ_C 67.3), and from H-8 (δ_H 2.50 and 2.59) to C-4 (δ_C 59.6)/C-6 (δ_C 67.3)/C-7 (δ_C 75.1) strongly supported the connection between the methyl group and partial structures via a triyne linkage. A careful comparison of ^{1}H NMR spectra of **2** with that of **1** revealed an addition of exchangeable proton signal at δ_H 2.60, assigned to 9-OH, and a difference in H-9 multiplicity (a pentet in **2** vs. a quartet in **1**) caused by additional ^{1}H–^{1}H coupling between H-9 and 9-OH in **2**. The relative configuration of **2** was inferred based on the high similarity of **1** and **2** in their ^{1}H and ^{13}C NMR chemical shifts and ^{1}H–^{1}H coupling constants. The specific rotation of **2** was measured as $[\alpha]_D^{30} - 3.71$ (*c* 0.1, CH_2Cl_2), very similar to that of **1** {$[\alpha]_D^{30} - 3.17$ (*c* 0.1, CH_2Cl_2)}. Thus, the absolute configurations of **2** were assigned as 9*R* and 10*R*. Previously, isolobetyol, a tetrahydropyran-bearing polyacetylene from *P. grandiflorum*, was reported with the *erythro* configuration for its 1-(tetrahydro-2*H*-pyran-2-yl)ethanol unit, based on NOESY correlations [8]. However, similarities in the ^{1}H and ^{13}C NMR spectra including chemical shifts and ^{1}H–^{1}H coupling constants of isolobetyol with compounds **1** and **2** suggested the relative configuration of 9*R** and 10*R** to be *threo* form.

Pilosulinene D (**3**) was purified as a white powder. The molecular formula of compound **3** was determined as $C_{16}H_{18}O_3$ by HR–ESI–MS at *m/z* 257.1187 $[M-H]^-$, indicating seven degrees of unsaturation (Supporting Information S1: Figure S15). The ^{1}H NMR spectrum showed signals for a methyl proton (δ_H 1.77), an oxygenated methine (δ_H 5.36), three aromatic protons (δ_H 7.24, 7.17, 6.98), a hydroxy proton (δ_H 5.65), and four olefinic protons (δ_H 6.89, 6.09, 6.07, 5.55). The ^{13}C NMR spectrum displayed signals for a methyl carbon (δ_C 19.0), a di-oxygenated methine (δ_C 101.8), ten sp2 carbons (δ_C 153.0, 141.9, 136.9, 134.0, 129.0, 121.9, 119.0, 117.2, 113.1, 110.4), and two unprotonated carbons (δ_C 97.1, 83.9) (Table 2 and Supporting Information S1: Figures S16 and S17). COSY spectrum showed the correlations of H-3 (δ_H 7.24) with H-2 (δ_H 7.17) and H-4 (δ_H 6.98), H-7 (δ_H 6.89) and H-8 (δ_H 6.07), as well as H-12 (δ_H 6.09) with H-11 (δ_H 5.55) and H-13 (δ_H 1.77) (Supporting Information S1: Figure S18). HMBC correlations from H-2 (δ_H 7.17) to C-6 (δ_C 121.9), from H-3 (δ_H 7.24) to C-1 (δ_C 136.9)/C-5 (δ_C 153.0), from H-4 (δ_H 6.98) to C-5 (δ_C 153.0)/C-6 (δ_C 121.9), from H-7 (δ_H 6.89) to C-1 (δ_C 136.9)/C-5 (δ_C 153.0)/C-9 (δ_C 83.9), and from H-13 (δ_H 1.77) to C-9 (δ_C 83.9)/C-10 (δ_C 97.1) supported the partial structure of an alkyne-substituted phenol (Figure 5 and Supporting Information S1: Figures S19 and S20). Additional HMBC correlations from H-14 (δ_H 5.36) to C-2 (δ_C 119.0)/C-6 (δ_C 121.9)/C-15 (δ_C 53.1)/C-16 (δ_C 53.1) suggested a di-*O*-methylated acetal at the C-1 position (Figure 5). The two vicinal coupling constants between H-7 and H-8 ($^3J_{H\text{-}7,\ H\text{-}8} = 11.4$ Hz), and between H-11 and H-12 ($^3J_{H\text{-}11,H\text{-}12} = 15.7$ Hz) indicated the *cis* configuration at H-7/H-8 and the *trans* configurations at H-11/H-12, respectively.

Pilosulinene C (**4**) was also isolated as a white powder. The molecular formula of compound **4** was determined to be

TABLE 2 | ^{1}H NMR data at 600 MHz and ^{13}C NMR data at 150 MHz of compounds **3–6** in $CDCl_3$ (δ in ppm, J in Hz).

	Compound 3		Compound 4		Compound 5		Compound 6	
No.	δ_C	δ_H	δ_C	δ_H	δ_C	δ_H	δ_C	δ_H
1	136.9		137.0		135.2		135.1	
2	119.0	7.17, dd (7.9, 1.1)	119.4	7.17, m	123.9	7.50, dd (7.8, 1.2)	123.9	7.46, d (7.7)
3	129.0	7.24, t (7.9)	128.6	7.17, m	129.6	7.39, t (7.8)	129.2	7.34, d (7.7)
4	117.2	6.98, dd (7.9, 1.1)	116.3	6.87, dd (6.1, 3.1)	122.2	7.22, dd (7.8, 1.2)	121.3	7.13, d (7.7)
5	153.0		153.4		152.3		153.8	
6	121.9		121.9		123.5		125.5	
7	134.0	6.89, d (11.4)	134.0	7.07, d (16.6)	132.7	7.06, d (11.5)	132.5	7.33, d (16.4)
8	113.1	6.07, dd (11.4, 2.0)	115.7	6.26, dd (16.6, 1.9)	115.0	6.21, dd (11.5, 2.4)	117.9	6.14, dd (16.4, 1.7)
9	83.9		86.7[a]		93.8		86.1	
10	97.1		91.5[a]		96.9		92.7	
11	110.4	5.55, dt (15.7, 2.0)	110.9	5.68, dt (15.7, 1.9)	110.0	5.52, dt (15.8, 1.8)	110.7	5.69, dt (15.8, 1.7)
12	141.9	6.09, dq (15.7, 6.9)	140.5	6.23, dq (15.7, 6.9)	141.9	6.10, dq (15.8, 6.9)	141.2	6.26, dq (15.8, 7.0)
13	19.0	1.77, dd (6.9, 2.0)	19.0	1.84, dd (6.9, 1.9)	18.5	1.77, dd (6.9, 1.8)	19.0	1.85, dd (7.0, 1.7)
14	101.8	5.36, s	101.6	5.38, s	192.7	10.11, s	192.1	10.15, s
15	53.1	3.30, s	53.3	3.31, s				
16	53.1	3.30, s	53.3	3.31, s				
5-OH		5.65, brs		5.30, brs		5.63, brs		5.44, brs

[a]Assigned by HMBC.

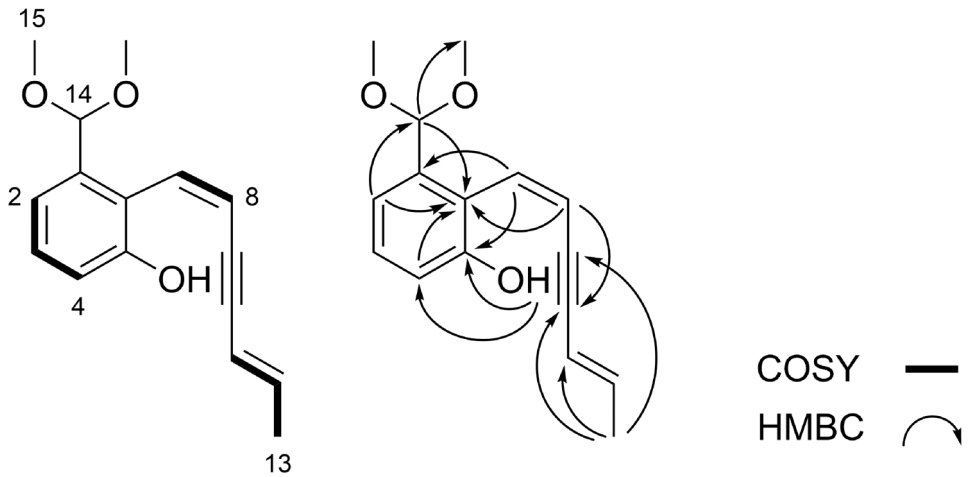

FIGURE 5 | Planar structure of **3** based on key COSY and HMBC correlations.

$C_{16}H_{18}O_3$ based on the deprotonated molecular ion found in HR–ESI–MS (*m/z* 257.1187 $[M–H]^-$) as shown in Supporting Information S1: Figure S21. The 1D NMR spectra of **4** are highly similar to those of **3** (Table 2 and Supporting Information S1: Figures S22–S26). The notable difference in the ^{1}H NMR spectrum of **4** was the larger ^{1}H–^{1}H vicinal coupling constant between H-7 and H-8 (16.6 Hz in **4**, 11.4 Hz in **3**), indicating a *trans* configuration for H-7/H-8 in **4**.

The acetal groups in **3** and **4** may have been converted from aldehydes through the addition of alcohols (Supporting Information S1: Figure S27). Therefore, compounds **3** and **4** could be artifacts generated during purification. Careful inspection of the LR-LC-MS data for the parent fraction (PG-H2) did not reveal peaks corresponding to **3** and **4** (*m/z* 257 $[M–H]^-$). However, peaks with *m/z* values of 211, corresponding to the respective aldehydes, were observed. This finding implied that extract or fraction was relatively less changeable than purified compound. It also supported that the potential formation of artifacts should be considered while alcohols was used in separation of aldehyde compounds. As a result, compound isolation was carried out using normal-phase chromatography under alcohol-free mobile phase conditions. This led to the isolation of the original aldehyde-containing compounds of **3** and **4**, identified as **5** and **6**, respectively. Spectroscopic data comparison identified compound **6** as a known polyacetylene, pilosulinene A [25].

Pilosulinene B (**5**) was found to have the same *m/z* value and a similar ^{1}H NMR spectrum to **6**. A detailed comparison of the ^{1}H NMR spectra of **5** and **6** (Table 2) indicated that the geometry between H-7 and H-8 in **5** was *cis* ($^{3}J_{H\text{-}7,H\text{-}8} = 11.5$ Hz), while in **6** it was *trans* ($^{3}J_{H\text{-}7,H\text{-}8} = 16.4$ Hz) (Supporting Information S1: Figures S28–S37).

The structures of other known analogs (**7**–**14**) were confirmed by careful comparison of their MS and NMR data along with specific rotations, to literature values. They were identified as 9*Z*,16*E*-octadeca-9,16-dien-12,14-diynoic acid (**7**) [26], α-dimorphecolic acid (**8**) [27], vanillin (**9**) [28], *E*−4-(3-ethoxyprop-1-en-1-yl)−2-methoxyphenol (**10**) [29], butyl ferulate (**11**) [30], 1-acetyl-β-carboline (**12**) [31], 1,1-dibutoxybutane (**13**) [32], and lobetyol (**14**) [33] (Supporting Information S1: Figures S38–S73).

Compounds **6**–**13** were isolated from the root of *P. grandiflorum* for the first time. Notably, compound **13** has primarily been reported as a synthetic additive for diesel fuel [32] and can be synthesized from butanal and butanol. However, butanol was never used during extraction, hexanes fraction preparation, or purification in this study, suggesting that compound **13** is naturally derived.

2.2 | Antimicrobial and Antifungal Activities of Isolated Compounds

An investigation into the antimicrobial and antifungal activities were evaluated against several strains of Gram-positive and Gram-negative bacteria together with fungal strains that are related to antimicrobial susceptibility studies. The results of the investigation for *P. grandiflorum* extracts and fractions revealed that the 70% EtOH extract and its hexanes fraction inhibited both *S. aureus* KCTC 1927 and *E. coli* KCTC 2441 (Supporting Information S1: Table S1). Furthermore, 12 compounds (**1**–**2**, **5**–**14**) were evaluated for antibacterial and antifungal activities, with results expressed as MIC (Table 3). Compounds **8**, **12**–**14** displayed potent antibacterial activities against Gram-positive *K. rhizophila* KCTC 1915 and *S. aureus* KCTC 1927, as well as Gram-negative *E. coli* KCTC 2441, and antifungal activities against *C. albicans* KCTC 7122, *C. glabrata* KCTC 7219, and *A. fumigatus* KCTC 6145. Compounds **1**–**2**, **5**, and **7** showed moderate antimicrobial activity against *S. aureus* KCTC 1927, while compounds **1** and **2** exhibited antifungal activity against *C. albicans* KCTC 7122. Additionally, anti-quorum sensing (QS) activity was tested with compounds **1**–**2**, **5**, **8**, and **12**–**14** against *Chromobacterium violaceum* KCTC 2897, a Gram-negative QS reporter strain widely used in quorum sensing inhibition assays. Novel compound **1** showed the strongest anti-QS activity between tested compounds in the qualitative screening of anti-QS activity using the disc diffusion assay by inhibition of violacein production as indicator of QS inhibition (Figure 6). Compound **1** also showed the highest anti-QS activity with a 39.6% inhibition of violacein production at 128 μg/mL. Compounds **2** and **14** exhibited weak inhibition (Supporting Information S1: Table S2). The antibacterial activities of **8** and **12** were previously reported [34, 35]; however, this study is the first report about their inhibitory effects on *K. rhizophila* KCTC 1915 and their antifungal activities. The antibacterial and antifungal activities of **13** and **14** were also revealed for the first time in this study. Collectively, compounds **1** and **2** are considered key contributors to the antimicrobial activities in *P. grandiflorum*.

TABLE 3 | Antibacterial and antifungal activities of isolated compounds.

Antibacterial activity		Compounds														
MIC (μg/mL)		1	2	5	6	7	8	9	10	11	12	13	14	Ampicillin	Vancomycin
Gram (+) bacteria	*B. subilis* KCTC 1021	> 128	> 128	> 128	> 128	> 128	> 128	> 128	> 128	> 128	> 128	> 128	> 128	0.5	0.25
	K. rhizophila KCTC1915	> 128	> 128	> 128	> 128	> 128	1	> 128	> 128	> 128	1	1	1	0.5	0.25
	S. aureus KCTC1927	8	8	8	> 128	4	2	> 128	> 128	> 128	0.5	0.5	0.5	0.25	> 128
Gram (−) bacteria	*E. coli* KCTC2441	> 128	> 128	> 128	> 128	> 128	1	> 128	> 128	> 128	1	1	1	4	> 128
	S. typhimurium KCTC2515	> 128	> 128	> 128	> 128	> 128	> 128	> 128	> 128	> 128	> 128	> 128	> 128	2	> 128
	K. pneumonia KCTC2690	> 128	> 128	> 128	> 128	> 128	> 128	> 128	> 128	> 128	> 128	> 128	> 128	> 128	> 128

Antifungal activity		Compounds													
MIC (μg/mL)		1	2	5	6	7	8	9	10	11	12	13	14	Cyclohexamide	
Pathogen fungi	*C. albicans*K KCTC 7122	0.25	1	> 128	> 128	> 128	0.25	> 128	> 128	> 128	0.25	0.25	0.25	0.25	
	C. glabrata KCTC7219	8	64	> 128	> 128	> 128	0.25	> 128	> 128	> 128	0.5	0.5	0.5	1	
	A. fumigatus KCTC6145	> 128	> 128	> 128	> 128	> 128	0.5	> 128	> 128	> 128	1	1	1	1	

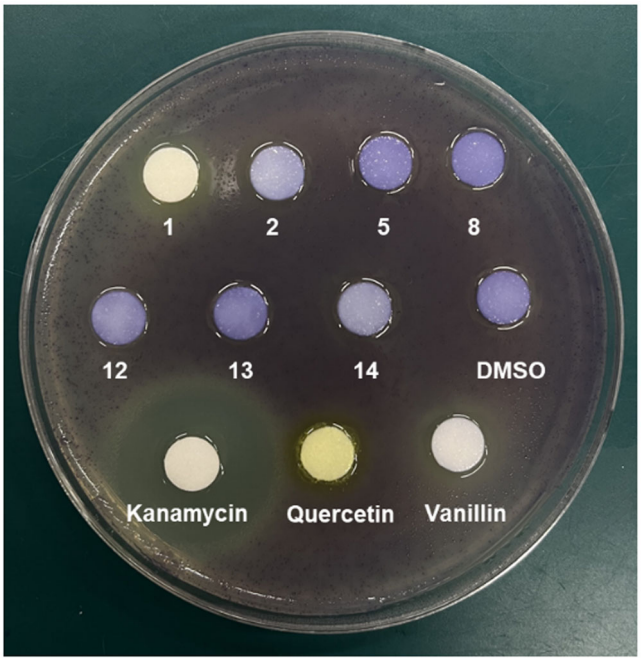

FIGURE 6 | Anti-QS screening results using disk diffusion assay.

3 | Conclusion

As a result, five novel polyacetylenes (**1**–**5**) were isolated from the root of the edible plant, *P. grandiflorum* (Campanulaceae), along with nine known compounds (**6**–**14**). Among the isolated known analogs, compounds **6**–**13** were first observed from this plant. In addition, the absolute configurations of platypyran A (**1**) were unambiguously assigned using *J*-based configuration analysis, ^{1}H–^{1}H coupling constant analysis, and Mosher's esterification of secondary alcohols. The family Campanulaceae have been reported as one of major producer of polyacetylenes [36]. All the novel polyacetylenes in this study had a C14 skeleton, supporting the view that *P. grandiflorum* is a major producer of C14 polyacetylenes. Polyacetylenes were reported with multiple pharmacological activities including antibacterial activities [36] and can be considered as a phytoalexins produced by the response to tissue damage or a pathogenic infection. Therefore, polyacetylenes could be attractive molecules for further studies on characteristic structure features related to antimicrobial activities. This study identified potential antimicrobial polyacetylenes (**1** and **2**) through evaluation of their antimicrobial and QS inhibitory activities and demonstrated the new pharmacological potentials of the compounds **8**, **12**, **13**, and **14**. In conclusion, this study expanded the chemical space of *P. grandiflorum* and provided insights into its potential antimicrobial principles, furthering its medicinal use.

4 | Experimental

4.1 | Chemistry

4.1.1 | General

Specific rotations were measured by a JASCO DIP-100 polarimeter (JASCO Co., Tokyo, Japan). NMR spectra were obtained on an AVANCE NEO 600 spectrometer (NFEC-2019-09-257998, Bruker Switzerland AG, Fällanden, Switzerland) at the Core Research Support Center for Natural Products and Medicinal Materials (CRCNM) and on Bruker AVANCE DPX 400 and DMX 250 spectrometers at the College of Pharmacy, Yeungnam University, with $CDCl_3$ (δ_C 77.16, δ_H 7.26) at 298 K. HR–FAB–MS spectra were recorded on a JMS-700 mass spectrometer (JEOL, Tokyo, Japan) with a 6890 Series GC system (Agilent Technologies, Santa Clara, CA, USA). HR–ESI–MS was measured using a Q Exactive UHMR Hybrid Quadrupole-Orbitrap MS system coupled with a Vanquish UHPLC (Thermo Fisher Scientific, Waltham, MA, USA) at the CRCNM. GCMS was recorded on a GCMS-QP2010 (Shimadzu, Kyoto, Japan). LR–ESI–MS spectra were measured using an Agilent 6120 mass spectrometer (Santa Clara, CA, USA) with a reversed-phase (RP) Phenomenex Luna 3μ C18(2) 100 Å column (150 × 4.6 mm). Vacuum liquid chromatography (VLC) and open-column chromatography were performed using 70–230 mesh silica gel (Merck). Medium-pressure liquid chromatography (MPLC) was performed using a Biotage Isolera One system (Uppsala, Sweden) with a Biotage SNAP KP-Sil 100-g silica column. HPLC isolation was conducted using a combination of a Waters 1525 binary pump/2487 dual-wavelength detector or a Waters 1525 binary pump/996 Photodiode Array (PDA) detector with an analytical or semi-preparative Hector M 5-micron C18 column (250 × 4.6 or 250 × 10 mm). Preparative HPLC was performed using on a Gilson 321 HPLC system (a 321 pump and UV/Vis-155 detector) with a preparative Hector M 5-micron C18 100 Å column (250 × 21.2 mm). Absorbance values for the QS inhibition assay were measured using a SpectraMax ABS Plus microplate reader (Molecular Devices, San Jose, CA, USA). The InChI codes of the investigated compounds, together with some biological activity data, are provided as Supporting Information.

4.1.2 | Plant Materials

The dried root of *P. grandiflorum* was prepared from Naemome Dah (Ulsan, Republic of Korea). The voucher specimen was identified and deposited by Dr. Hyukjae Choi at the Pharmacognosy Laboratory, Yeungnam University, Gyeongsan, Korea.

4.1.3 | Extraction and Isolation

The dried roots of *P. grandiflorum* (9.5 kg) were extracted three times using 70% EtOH (30 L) at room temperature (RT) for 3 days. The combined extract was evaporated to yield 2.5 kg of black gummy crude extract. The dried extract (2.0 kg) was suspended in deionized water (3.5 L) and successively extracted three times with 5.0 L of hexanes, dichloromethane (DCM), ethyl acetate (EtOAc), and *n*-butanol (*n*-BuOH), respectively, and then concentrated to yield fractions of hexanes (PG-H, 3.3 g), DCM (PG-D, 25.4 g), EtOAc (PG-E, 31.8 g), *n*-BuOH (PG-B, 154.0 g), and water (PG-W, 2.3 kg). A portion of the hexanes fraction (3.0 g) was separated into 10 subfractions (PG-H1–PG-H10) by normal-phase (NP) MPLC with following conditions; Biotage SNAP KP-Sil 100 g column, a linear gradient of mixtures with DCM and MeOH from 100:0 to 0:100. PG-H1 (**13**, 1018.2 mg) was further separated via MPLC. A portion of the fraction PG-H2 (23.1 mg) was subjected to reversed-phase (RP) preparative HPLC (Hector M 5 micron C18 100 Å, 250 × 21.2 mm) under isocratic conditions of H_2O:ACN (61:39) to yield compounds **3** (0.5 mg, t_R = 12.5 min)

and **4** (1.0 mg, $t_R = 18.0$ min). The remaining PG-H2 fraction was further separated by NP analytical HPLC (Hector M Sil 5 micron, 250 × 4.6 mm) under isocratic conditions of hexanes:EtOAc (75:25), yielding fraction PG-H2-A (6.5 mg, $t_R = 19.5$ min), **5** (3.9 mg, $t_R = 20.5$ min), and **11** (2.6 mg, $t_R = 21.5$ min). Fraction PG-H2-A was applied further isolation by NP analytical HPLC (Hector M Sil 5 micron, 250 × 4.6 mm) under isocratic conditions of hexanes:EtOAc (85:15) to get **6** (2.5 mg, $t_R = 35.2$ min). Fractions PG-H4–H6 (282.9 mg) were combined and subjected to RP semipreparative HPLC with Hector M 5 micron C18 100 Å column (250 × 10 mm) and step gradient elution of water and acetonitrile (50:50–0:100) to afford compounds **1** (32.4 mg) and **2** (5.3 mg). Subfraction PG-H4H (1.6 mg) was further separated by RP HPLC (Hector M 5 micron C18 100 Å, 250 × 4.6 mm) to yield compound **7** (0.5 mg). PG-H9 was chromatographed via RP semipreparative HPLC (Hector M 5 micron C18 100 Å, 250 × 10 mm) under isocratic conditions with 65% acetonitrile in deionized water, yielding compound **8** (2.0 mg). PG-H3 (222.5 mg) was fractionated by silica gel open-column chromatography (column size: 1.8 × 23 cm) by step gradient mixtures of hexanes and EtOAc (100:0–0:100) to yield compound **9** (9.6 mg). The second extraction of the dried roots of *P. grandiflorum* (9.5 kg) followed the same method as the first, and the extract was evaporated in vacuo, yielding a black gummy extract (2.3 kg). The dried extract (1.9 kg) was dissolved in water and successively extracted with hexanes, DCM, EtOAc, and *n*-BuOH, and then concentrated to yield hexanes (PG2-H, 3.6 g), DCM (PG2-D, 20.0 g), EtOAc (PG2-E, 12.6 g), *n*-BuOH (PG2-B, 176.2 g), and water (PG2-W, 2.1 kg) fractions, respectively. A portion of the hexanes layer (3.0 g) was fractionated into eight fractions (PG2-H1–PG2-H8) via MPLC using a silica column (Biotage SNAP KP-Sil 100 g) following similar chromatographic methods with PG-1 as a linear gradient of DCM:MeOH (100:0–0:100). PG2-H3 was chromatographed via RP semipreparative HPLC with a Hector M 5 micron C18 column (250 × 10 mm) by a step gradient of acetonitrile and water (45:55–100:0), yielding compounds **10** (3.2 mg) and **12** (5.0 mg). The DCM layer (11.9 g) was fractionated into nine fractions (PG-D1–PG-D9) via silica gel VLC using a step gradient of hexanes and EtOAc (100:0–0:100) and EtOAc:MeOH (75:25–0:100). Fraction PG-D7 (600.0 mg) was separated into 12 fractions (PG-D7A–PG-D7L) via silica open-column chromatography using a step gradient of DCM:MeOH (100:0–0:100). PG-D7J (99.9 mg) was purified by RP preparative HPLC (Hector M 5 micron C18 100 Å, 250 × 21.2 mm) under isocratic conditions with 35% acetonitrile to elute compound **14** (35.9 mg).

Platypyran A (**1**): Brown oil; $[\alpha]_D^{30} - 3.17$ (*c* 0.1, CH_2Cl_2); HR–FAB–MS obsd. *m/z* 219.1391 $[M+H]^+$, calcd. for $C_{14}H_{18}O_2^+$, 219.1380; ^1H and ^{13}C NMR, see Table 1.

Platypyran B (**2**): Yellow oil; $[\alpha]_D^{30} - 3.71$ (*c* 0.1, CH_2Cl_2); HR–FAB–MS obsd. *m/z* 217.1228 $[M+H]^+$, calcd. for $C_{14}H_{16}O_2^+$, 217.1223; ^1H and ^{13}C NMR, see Table 1.

Pilosulinene D (**3**): White powder; HR–ESI–MS obsd. *m/z* 257.1187 $[M-H]^-$, calcd. for $C_{16}H_{18}O_3^-$, 257.1183; ^1H and ^{13}C NMR, see Table 2.

Pilosulinene C (**4**): White powder; HR–ESI–MS obsd. *m/z* 257.1184 $[M-H]^-$, calcd. for $C_{16}H_{18}O_3^-$, 257.1183; ^1H and ^{13}C NMR, see Table 2.

Pilosulinene B (**5**): White powder; HR–ESI–MS obsd. *m/z* 211.0759 $[M-H]^-$, calcd. for $C_{14}H_{11}O_2^-$, 211.0765; ^1H and ^{13}C NMR, see Table 2.

4.1.4 | Advanced Mosher's Method

Two samples of compound **1** (2 mg each) were prepared. To one vial, a catalytic amount of 4-dimethylaminopyridine (Sigma-Aldrich, St. Louis, MO, USA), 20 μL of *S*-(+)-α-methoxy-α-(trifluoromethyl)phenylacetyl chloride (*S*-MTPA Cl) (Sigma-Aldrich, St. Louis, MO, USA), and pyridine-d_5 (0.7 mL) were added. The vial was sealed and reacted for 16 h at 40°C with stirring. The other vial of **1** was derivatized with *R*-MTPA Cl (Sigma-Aldrich, St. Louis, MO, USA) following the same procedure. The resulting products were dried under a N_2 stream. The evaporated materials were suspended in deionized water (1 mL) respectively, and Mosher's ester products of **1** were extracted with *n*-hexane (1 mL × 3). The combined *n*-hexane layers were evaporated to give the *S*/*R*-MTPA esters of **1**, and their ^1H NMR spectra were measured to assign the absolute configuration of C-9 by calculating $\Delta\delta_{S-R}$ values [24].

4.2 | Antimicrobial and Quorum-Sensing Inhibitory Activities

4.2.1 | Minimum Inhibitory Concentration (MIC) Against Bacteria and Fungi

The antibacterial and antifungal activities were tested on six bacterial strains (*Bacillus subtilis* KCTC1021, *Escherichia coli* KCTC2441, *Klebsiella pneumonia* KCTC 2690, *Kocuria rhizophila* KCTC1915, *Salmonella typhimurium* KCTC 2515, and *Staphylococcus aureus* KCTC1927) and three fungal strains (*Candida albicans* KCTC 7122, *Candida glabrata* KCTC 7219, and *Aspergillus fumigatus* KCTC 6145). These strains were selected as representative Gram-positive and Gram-negative bacteria and clinically relevant fungal pathogens, widely employed in antimicrobial susceptibility studies. These strains were inoculated in Muller–Hinton Broth (BD Difco) at 37°C for 24 h and calibrated to a McFarland standard of 0.5 (equivalent to 1.5×10^8 cfu/mL). The test samples and positive controls were prepared in DMSO at a concentration of 10 mg/mL. The stock solutions of compounds were then serially diluted twofold using Muller–Hinton Broth in 96-well plates to a concentration range of 256–0.5 μg/mL. Then, 50 μL of bacterial cultures was added to each well, resulting in a final sample concentration range as 128–0.25 μg/mL. The total inoculum concentration was 5.0×10^5 cfu/mL. After the incubation of 96-well plate at 37°C for 24 h, the MIC was evaluated by the observation of visible bacterial growth inhibition. Ampicillin and vancomycin served as positive controls for antibacterial activity, while cycloheximide was used as the positive control for antifungal activity [37].

4.2.2 | Qualitative Screening of QS Inhibitory Activity

A disc diffusion assay was performed to test QS inhibitory activity by measuring the inhibition of violacein pigment production of the isolates, except for compounds **3**, **4**, **6**, **7**, **9**, **10**, and **11**

(due to quantity limitations), with a previously described method with a minor modification [38]. The strain, *C. violaceum* KCTC 2897, was used as the reporter strain to assess anti-QS. Briefly, 5 mL of an overnight culture of the reporter strain was added to 45 mL LB medium containing 0.3% agar, and the mixture was cooled to approximately 45°C. The suspension was then added to the plates and left to solidify. Sterile filter paper discs (5 mm in diameter) were evenly placed on the surface of the LB agar. The test samples and reference compounds were dissolved in DMSO at a concentration of 10 mg/mL, and 20 μL of each solution was applied to the discs. The plates were incubated at 37°C for 18 h. DMSO was used as the negative control, while kanamycin, quercetin, and vanillin served as positive controls for QS inhibition [39, 40]. The anti-QS effect was evaluated by observing the absence of violacein pigmentation on the discs.

4.2.3 | Quantitative Analysis of QS Inhibitory Activity

The 96-well plate assay was employed to evaluate QS inhibitory activity of the isolates, except for compounds **3**, **4**, **6**, **7**, **9**, **10**, and **11**. The assay was conducted using *C. violaceum* KCTC 2897 cultured in LB broth, along with positive and negative controls. Vanillin and quercetin were used as QS inhibition (positive) controls [39, 40]. The protocol was slightly modified from previously published studies [38]. Test samples and controls were dissolved in DMSO at a stock concentration of 10 mg/mL. The stock solutions were serially diluted twofold in liquid LB medium to achieve a concentration range of 256 to 0.5 μg/mL in the 96-well plate. Subsequently, 50 μL of calibrated bacterial suspension was added to each well, resulting in a final concentration range of 128 to 0.25 μg/mL for the test samples. The final bacterial inoculum was adjusted to 5.0×10^5 CFU/mL. Plate was incubated at 37°C for 20 h, depending on the microbial strains. After incubation, 100 μL from each well was transferred to microcentrifuge tubes and centrifuged at 13,000 rpm for 10 min to precipitate violacein. The resulting pellets were resuspended in 200 μL of 1 × PBS and subjected to sonication for 30 s to extract violacein. The lysates were then centrifuged again at 13,000 rpm for 10 min to remove cell debris. Subsequently, 100 μL of the violacein-containing supernatant was transferred to a 96-well plate, and the absorbance was measured at 585 nm using a microplate spectrophotometer. All experiments were conducted in three independent trials, each performed in triplicate.

Acknowledgments

This study was supported by the Basic Science Research Program of the National Research Foundation of Korea (NRF) grants funded by the Ministry of Science and ICT (Grant No. RS-2020-NR049591, and RS-2021-NR-058513), [Cooperative Research Program for Agriculture Science & Technology Development (PJ014208032023) funded by Rural Development Administration], the Korea Basic Science Institute (National Research Facilities and Equipment Center) grant funded by the Ministry of Education (Grant No. RS-2025-02317758) and Yeungnam University research grant funded by Yeungnam University.

Conflicts of Interest

The authors declare no conflicts of interest.

Data Availability Statement

The data that supports the findings of this study are available in the supporting material of this article.

References

1. L. Zhang, X. Wang, J. Zhang, D. Liu, and G. Bai, "Ethnopharmacology, Phytochemistry, Pharmacology and Product Application of *Platycodon grandiflorum*: A Review," *Chinese Herbal Medicines* 16 (2024): 327–343, https://doi.org/10.1016/j.chmed.2024.01.005.

2. Y. Zhang, M. Sun, Y. He, et al., "Polysaccharides From *Platycodon grandiflorum*: A Review of Their Extraction, Structures, Modifications, and Bioactivities," *International Journal of Biological Macromolecules* 271 (2024): 132617, https://doi.org/10.1016/j.ijbiomac.2024.132617.

3. T. Goto, H. Tadao Kondo, H. Tamura, K. Kawahori, and H. Hattori, "Structure of Platyconin, a Diacylated Anthocyanin Isolated From the Chinese Bell-Flower *Platycodon grandiflorum*," *Tetrahedron Letters* 24 (1983): 2181–2184, https://doi.org/10.1016/S0040-4039(00)81877-8.

4. A. Inada, H. Murata, M. Somekawa, and T. Nakanishi, "Phytochemical Studies of Seeds of Medicinal Plants. II. A New Dihydroflavonol Glycoside and a New 3-Methyl-1-butanol Glycoside From Seeds of *Platycodon grandiflorum* A. DE CANDOLLE," *Chemical and Pharmaceutical Bulletin* 40 (1992): 3081–3083, https://doi.org/10.1248/cpb.40.3081.

5. J. Y. Lee, J. W. Yoon, C. T. Kim, and S. T. Lim, "Antioxidant Activity of Phenylpropanoid Esters Isolated and Identified From *Platycodon grandiflorum* A. DC," *Phytochemistry* 65 (2004): 3033–3039, https://doi.org/10.1016/j.phytochem.2004.08.030.

6. B. Chen, Z. Liu, Y. Zhang, et al., "Application of High-Speed Counter-Current Chromatography and HPLC to Separate and Purify of Three Polyacetylenes From *Platycodon grandiflorum*," *Journal of Separation Science* 41 (2018): 789–796, https://doi.org/10.1002/jssc.201700767.

7. J. C. Ahn, B. Hwang, H. Tada, K. Ishimaru, K. Sasaki, and K. Shimomura, "Polyacetylenes in Hairy Roots of *Platycodon grandiflorum*," *Phytochemistry* 42 (1996): 69–72, https://doi.org/10.1016/0031-9422(95)00849-7.

8. W. Li, "Isolobetyol, a New Polyacetylene Derivative From *Platycodon grandiflorum* Root," *Natural Product Research* 36, no. 1 (2022): 466–469, https://doi.org/10.1080/14786419.2020.1779269.

9. L. Zhang, Y. Wang, D. Yang, et al., "*Platycodon grandiflorus* —An Ethnopharmacological, Phytochemical and Pharmacological Review," *Journal of Ethnopharmacology* 164 (2015): 147–161, https://doi.org/10.1016/j.jep.2015.01.052.

10. L. L. Zhang, M. Y. Huang, Y. Yang, et al., "Bioactive Platycodins From Platycodonis Radix: Phytochemistry, Pharmacological Activities, Toxicology and Pharmacokinetics," *Food Chemistry* 327 (2020): 127029, https://doi.org/10.1016/j.foodchem.2020.127029.

11. Y. H. Choi, D. S. Yoo, M. R. Cha, et al., "Antiproliferative Effects of Saponins From the Roots of *Platycodon grandiflorumon* Cultured Human Tumor Cells," *Journal of Natural Products* 73 (2010): 1863–1867, https://doi.org/10.1021/np100496p.

12. L. Zhang, Z. H. Liu, and J. K. Tian, "Cytotoxic Triterpenoid Saponins From the Roots of *Platycodon grandiflorum*," *Molecules* 12 (2007): 832–841, https://doi.org/10.3390/12040832.

13. K. J. Jang, H. K. Kim, M. H. Han, et al., "Anti-Inflammatory Effects of Saponins Derived From the Roots of *Platycodon grandiflorus* in Lipopolysaccharide-Stimulated BV2 Microglial Cells," *International Journal of Molecular Medicine* 31 (2013): 1357–1366, https://doi.org/10.3892/ijmm.2013.1330.

14. H. L. Kim, J. Park, H. Park, et al., "*Platycodon grandiflorum* A. De Candolle Ethanolic Extract Inhibits Adipogenic Regulators in 3T3-L1 Cells and Induces Mitochondrial Biogenesis in Primary Brown Preadipocytes," *Journal of Agricultural and Food Chemistry* 63 (2015): 7721–7730, https://doi.org/10.1021/acs.jafc.5b01908.

15. M. Y. Ji, A. Bo, M. Yang, et al., "The Pharmacological Effects and Health Benefits of *Platycodon grandiflorus*—A Medicine Food Homology Species," *Foods* 9 (2020): 142, https://doi.org/10.3390/foods9020142.

16. J. Y. Lee, W. I. Hwang, and S. T. Lim, "Antioxidant and Anticancer Activities of Organic Extracts From *Platycodon grandiflorum* A. De Candolle Roots," *Journal of Ethnopharmacology* 93 (2004): 409–415, https://doi.org/10.1016/j.jep.2004.04.017.

17. T. Khanal, J. H. Choi, Y. P. Hwang, Y. C. Chung, and H. G. Jeong, "Saponins Isolated From the Root of *Platycodon grandiflorum* Protect Against Acute Ethanol-Induced Hepatotoxicity in Mice," *Food and Chemical Toxicology* 47 (2009): 530–535, https://doi.org/10.1016/j.fct.2008.12.009.

18. K. S. Kim, O. Ezaki, S. Ikemoto, and H. Itakura, "Effects of *Platycodon grandiflorum* Feeding on Serum and Liver Lipid Concentrations in Rats With Diet-Induced Hyperlipidemia," *Journal of Nutritional Science and Vitaminology* 41 (1995): 485–491, https://doi.org/10.3177/jnsv.41.485.

19. Y. Xie, H. Pan, H. Sun, and D. Li, "A Promising Balanced Th1 and Th2 Directing Immunological Adjuvant, Saponins From the Root of *Platycodon grandiflorum*," *Vaccine* 26 (2008): 3937–3945, https://doi.org/10.1016/j.vaccine.2008.01.061.

20. J. Kim, "Antibacterial and Anti-Inflammatory Effects of *Platycodon grandiflorum* Extracts," *Journal of Digital Convergence* 12 (2014): 359–366, https://doi.org/10.14400/JDC.2014.12.3.359.

21. I. S. Lee, M. C. Choi, and H. Y. Moon, "Effect of *Platycodon grandiflorum* A. DC Extract on the Bronchus Diseases Bacteria," *Korean Society for Biotechnology and Bioengineering Journal* 15 (2000): 162–166.

22. N. Matsumori, D. Kaneno, M. Murata, H. Nakamura, and K. Tachibana, "Stereochemical Determination of Acyclic Structures Based on Carbon−Proton Spin-Coupling Constants. A Method of Configuration Analysis for Natural Products," *Journal of Organic Chemistry* 64 (1999): 866–876, https://doi.org/10.1021/jo981810k.

23. Y. Ahn and T. Cohen, "A General Diastereoselective Synthesis of Spiroacetals Related to Those in Ionophores via the Reaction of Lactones With Cerium(III).Gamma. Cerioalkoxide. MAD Reverses the Diastereoselectivity of the Addition of Methylmetallics to a .beta.-Keto Ether," *Journal of Organic Chemistry* 59 (1994): 3142–3150, https://doi.org/10.1021/jo00090a036.

24. K. Fujii, Y. Ikai, H. Oka, M. Suzuki, and K. Harada, "A Non-empirical Method Using LC/MS for Determination of the Absolute Configuration of Constituent Amino Acids in a Peptide: Combination of Marfey's Method With Mass Spectrometry and Its Practical Application," *Analytical Chemistry* 69 (1997): 5146–5151, https://doi.org/10.1021/ac970289b.

25. R. Y. Wang, P. J. Su, B. Li, et al., "Two New Aromatic Derivatives From *Codonopsis pilosula* and Their α-Glucosidase Inhibitory Activities," *Natural Product Research* 36 (2022): 4929–4935, https://doi.org/10.1080/14786419.2021.1912749.

26. K. Oka, F. Saito, T. Yasuhara, and A. Sugimoto, "The Allergens of *Dendropanax trifidus* Makino and *Fatsia Japonica* Decne. et Planch. and Evaluation of Cross-Reactions With Other Plants of the Araliaceae Family," *Contact Dermatitis* 40 (1999): 209–213, https://doi.org/10.1111/j.1600-0536.1999.tb06036.x.

27. S. V. Naidu, P. Gupta, and P. Kumar, "Enantioselective Syntheses of (−)-Pinellic Acid, α- and β-Dimorphecolic Acid," *Tetrahedron* 63 (2007): 7624–7633, https://doi.org/10.1016/j.tet.2007.05.047.

28. S. Annen, T. Zweifel, F. Ricatto, and H. Grützmacher, "Catalytic Aerobic Dehydrogenative Coupling of Primary Alcohols and Water to Acids Promoted by a Rhodium(I) Amido N-Heterocyclic Carbene Complex," *ChemCatChem* 2 (2010): 1286–1295, https://doi.org/10.1002/cctc.201000100.

29. F. Wang, H. M. Hua, X. Bian, Y. H. Pei, and Y. K. Jing, "Two New Aromatic Compounds From the Resin of *Styrax tonkinensis* (Pier.) Craib," *Journal of Asian Natural Products Research* 8 (2006): 137–141, https://doi.org/10.1080/10286020500480712.

30. J. Chen, L. Zhang, P. Zhao, G. Ma, Q. Li, and X. Yu, "Synthesized Alkyl Ferulates With Different Chain Lengths Inhibited the Formation of Lipid Oxidation Products in Soybean Oil During Deep Frying," *Food Chemistry* 410 (2023): 135458, https://doi.org/10.1016/j.foodchem.2023.135458.

31. H. J. Shin, H. S. Lee, and D. S. Lee, "The Synergistic Antibacterial Activity of 1-Acetyl-Beta-Carboline and Beta-Lactams Against Methicillin-Resistant *Staphylococcus aureus* (MRSA)," *Journal of Microbiology and Biotechnology* 20 (2010): 501–505, https://doi.org/10.4014/jmb.0910.10019.

32. I. I. Yoeswono and T. Falah, "1,1-Dibutoxybutane as a Petroleum Diesel Fuel Blending Component and Their Mixture Performance," *Journal of Energy and Power Engineering* 10 (2016): 726, https://doi.org/10.17265/1934-8975/2016.12.002.

33. M. Ma, M. Wu, B. Tian, et al., "Polyacetylenes With Xanthine Oxidase Inhibitory Activity From the Medicinal and Edible Fruits of *Cyclocodon lancifolius* (Roxburgh) Kurz," *Fitoterapia* 170 (2023): 105631, https://doi.org/10.1016/j.fitote.2023.105631.

34. J. M. McRae, Q. Yang, R. J. Crawford, and E. A. Palombo, "Antibacterial Compounds From *Planchonia careya* Leaf Extracts," *Journal of Ethnopharmacology* 116 (2008): 554–560, https://doi.org/10.1016/j.jep.2008.01.007.

35. O. Kenny, N. P. Brunton, D. Walsh, C. M. Hewage, P. McLoughlin, and T. J. Smyth, "Characterisation of Antimicrobial Extracts From Dandelion Root (*Taraxacum officinale*) Using LC-SPE-NMR," *Phytotherapy Research* 29 (2015): 526–532, https://doi.org/10.1002/ptr.5276.

36. Q. Xie and C. Wang, "Polyacetylenes in Herbal Medicine: A Comprehensive Review of Its Occurrence, Pharmacology, Toxicology, and Pharmacokinetics (2014–2021)," *Phytochemistry* 201 (2022): 113288, https://doi.org/10.1016/j.phytochem.2022.113288.

37. I. Wiegand, K. Hilpert, and R. E. W. Hancock, "Agar and Broth Dilution Methods to Determine the Minimal Inhibitory Concentration (MIC) of Antimicrobial Substances," *Nature Protocols* 3 (2008): 163–175, https://doi.org/10.1038/nprot.2007.521.

38. N. K. Vijayan, H. Tanimu, and B. O. Sukumaran, "Comparative Study on Quorum Modulatory Effect of Selected Medicinal Plants on *Chromobacterium Violaceum* ATCC 12472 (MTCC 2656)," *Journal of Pure and Applied Microbiology* 18 (2024): 1848–1859, https://doi.org/10.22207/JPAM.18.3.34.

39. M. Skogman, S. Kanerva, S. Manner, P. Vuorela, and A. Fallarero, "Flavones as Quorum Sensing Inhibitors Identified by a Newly Optimized Screening Platform Using *Chromobacterium violaceum* as Reporter Bacteria," *Molecules* 21 (2016): 1211, https://doi.org/10.3390/molecules21091211.

40. D. Deryabin and A. Tolmacheva, "Antibacterial and Anti-Quorum Sensing Molecular Composition Derived From Quercus Cortex (Oak Bark) Extract," *Molecules* 20 (2015): 17093–17108, https://doi.org/10.3390/molecules200917093.

Supporting Information

Additional supporting information can be found online in the Supporting Information section.